

Flexible and Shape-Selective Guest Binding at Cu^{II} Axial Sites in 1-Dimensional Cu^{II}–1,2-Bis(4-pyridyl)ethane Coordination PolymersShin-ichiro Noro,^{*,†} Satoshi Horike,[‡] Daisuke Tanaka,[‡] Susumu Kitagawa,[‡] Tomoyuki Akutagawa,[†] and Takayoshi Nakamura[†]*Research Institute for Electronic Science, Hokkaido University, Sapporo 060-0812, Japan, and Department of Synthetic Chemistry and Biological Chemistry, Graduate School of Engineering, Kyoto University, Katsura, Nishikyo-ku, Kyoto 615-8510, Japan*

Received May 26, 2006

A series of guest-binding Cu^{II} coordination polymers, {[Cu(bpetha)₂(acetone)₂]·2PF₆}_n (bpetha = 1,2-bis(4-pyridyl)ethane) (1), {[Cu(bpetha)₂(DMF)₂]·2PF₆}_n (2), {[Cu(bpetha)₂(MeCN)₂]·2PF₆·2MeCN}_n (3), {[Cu(bpetha)₂(H₂O)₂]·2PF₆·3THF·2H₂O}_n (4), {[Cu(bpetha)₂(H₂O)₂]·2PF₆·3dioxane}_n (5), and {[Cu(bpetha)₂(H₂O)₂]·2PF₆·2-PrOH·2H₂O}_n (6), have been synthesized and crystallographically characterized. Their framework stabilities and guest-exchange properties have also been investigated. All compounds form a similar framework motif, a “double chain”, in which the bpetha ligands bridge Cu^{II} centers to form 1-D [Cu(bpetha)₂]_n double chains. A variety of Lewis base guest molecules, such as H₂O, acetone, DMF, MeCN, THF, dioxane, and 2-PrOH, are incorporated into the assembly of the 1-D double chains. These chains flexibly change their forms of assembly in a guest-dependent manner. Interestingly, acetone, DMF, and MeCN guests with a carbonyl or cyanide group coordinate directly to the axial sites of the Cu^{II} centers; in contrast, THF, dioxane, and 2-PrOH guests with an ether or alcohol group are incorporated into the frameworks not via coordination bonds but via weak interactions (hydrogen bonds and van der Waals forces). This selectivity is probably due to steric effects at coordinated oxygen or nitrogen atoms of the guests. Crystal-to-crystal transformations triggered by guests are observed, during which guests coordinated to the Cu^{II} axial sites are readily removed and replaced by other guests.

Introduction

A new class of porous materials known as coordination polymers, constructed from transition metal ions and organic bridging ligands as connectors and linkers, respectively, have attracted a great deal of attention recently, and considerable research effort has been devoted to the development, design, and synthesis of novel porous metal–organic frameworks.^{1,2} In such porous frameworks, guest molecules ordinarily encounter no stronger interactions than attractive van der Waals forces from pore walls. In contrast, guests with the ability to engage in special interactions such as hydrogen

bonding and π – π interactions are incorporated at corresponding special sites of pore walls. These host–guest specific interactions can induce selectivity in porous frameworks.³

* To whom correspondence should be addressed. E-mail: noro@es.hokudai.ac.jp.

[†] Hokkaido University.

[‡] Kyoto University.

- (1) (a) Kitagawa, S.; Noro, S. In *Comprehensive Coordination Chemistry II: From Biology to Nanotechnology*; McCleverty, J. A., Meyer, T. J., Eds.; Pergamon Press: Oxford, U.K., 2003; Vol. 7, pp 231–261. (b) Kitagawa, S.; Kitaura, R.; Noro, S. *Angew. Chem., Int. Ed.* **2004**, *43*, 2334–2375. (c) Uemura, K.; Kitagawa, S. *Chem. Soc. Rev.* **2005**, *34*, 109–119.

- (2) (a) Oh, M.; Carpenter, G. B.; Sweigart, D. A. *Acc. Chem. Res.* **2004**, *37*, 1–11. (b) Yaghi, O. M.; O’Keeffe, M.; Ockwig, N. W.; Chae, H. K.; Eddaoudi, M.; Kim, J. *Nature (London)* **2003**, *423*, 705–714. (c) Janiak, C. *J. Chem. Soc., Dalton Trans.* **2003**, 2781–2804. (d) James, S. L. *Chem. Soc. Rev.* **2003**, *32*, 276–288. (e) Moulton, B.; Zaworotko, M. J. *Curr. Opin. Solid State Mater. Sci.* **2002**, *6*, 117–123. (f) Kim, K. *Chem. Soc. Rev.* **2002**, *31*, 96–107. (g) Evans, O. R.; Lin, W. *Acc. Chem. Res.* **2002**, *35*, 511–522. (h) Moulton, B.; Zaworotko, M. J. *Chem. Rev.* **2001**, *101*, 1629–1658. (i) Kesaneli, B.; Lin, W. *Coord. Chem. Rev.* **2003**, *246*, 305–326. (j) Tong, M.-L.; Chen, H.-J.; Chen, X.-M. *Inorg. Chem.* **2000**, *39*, 2235–2238. (k) Férey, G.; Mellot-Draznieks, C.; Serre, C.; Millange, F.; Dutour, J.; Surlé, S.; Margiolaki, I. *Science* **2005**, *309*, 2040–2042. (l) Rosseinsky, M. J. *Microporous Mesoporous Mater.* **2004**, *73*, 15–30. (m) Lee, E. Y.; Jang, S. Y.; Suh, M. P. *J. Am. Chem. Soc.* **2005**, *127*, 6374–6381. (n) Abrahams, B. F.; Moylan, M.; Orchard, S. D.; Robson, R. *Angew. Chem., Int. Ed.* **2003**, *42*, 1848–1851. (o) Mori, W.; Takamizawa, S.; Nozaki-Kato, C.; Ohmura, T.; Sato, T. *Microporous Mesoporous Mater.* **2004**, *73*, 31–46. (p) Ohmori, O.; Kawano, M.; Fujita, M. *Angew. Chem., Int. Ed.* **2005**, *44*, 1962–1964.

Another special interaction site can be introduced by the immobilization of guest-binding metal centers (MCs) into porous frameworks.⁴ Because MCs can interact with Lewis base guests through coordination bonds having an energy (ca. 10^2 kJ mol⁻¹) much greater than that of dispersion forces (<5 kJ mol⁻¹) or hydrogen bonds (ca. 10–40 kJ mol⁻¹), they can show highly selective incorporation of guests as efficiently as hydrogen bonding sites. In addition, microporous coordination polymers with guest-binding MCs can function as chromic sensors and flexible frameworks, because ligation and release of the MCs' guests often influence the coordination geometry or splitting of the d orbitals.⁵ Moreover, it is well-known that a variety of transition metal ions can function as active centers in catalyzed reactions. A combination of MC characteristics and traditional porous properties (shape- and size-selectivity) can be used to create desired, highly efficient, tailor-made properties. Immobilization of an MC into a porous host has been attempted with zeolites, polymeric matrixes, and clays by ion exchange, impregnation, or isomorphous substitution.⁶ However, in these cases, the isolation and uniformity of MCs was insufficient and the environment surrounding the MCs was not well understood. If an MC can be directly incorporated onto the surface of a channel, a completely isolated and uniform arrangement can be realized. Hence, it is important to establish synthetic methods for the immobilization of MCs onto the pore surface of microporous coordination polymers.

Several attempts have been made to create guest-binding MCs in microporous coordination polymers. For example, lanthanide ions that have a large coordination number (from 7 to 10) and polyhedral coordination geometry tend to facilitate the coordination of volatile molecules and are therefore good candidates for the construction of guest-binding MCs.⁷ Multinuclear metal clusters can also provide an opportunity to create guest-binding MCs in extended frameworks. In this system, the geometric constraints placed on the metal center by virtue of extensive multidentate ligand bonding often allow a volatile terminal ligand to occupy a coordination site on the metal ion.⁸

We have recently focused on a Cu^{II} ion displaying Jahn–Teller distortion as a good building block for the formation of guest-binding MCs.^{4,9} Due to ligand field effects, the binding of the axial ligand to a Cu^{II} ion is sufficiently weak to allow its ready release. In addition, the resulting geometry (square planar) is stable. Hence, Cu^{II} centers can freely catch and release Lewis base guests, responding to a change in the external environment.

Several porous coordination polymers capable of creating guest-binding Cu^{II} centers have been reported to date.^{5b,8c,9,10} However, there are few examples of guest selectivity at Cu^{II} centers.^{9c} In this paper, we provide the first detailed report on guest selectivity at Cu^{II} axial sites in a series of guest-binding coordination polymers: {[Cu(bpetha)₂(acetone)₂]}·2PF₆ (1), {[Cu(bpetha)₂(DMF)₂]}·2PF₆ (2), {[Cu(bpetha)₂(MeCN)₂]}·2PF₆·2MeCN (3), {[Cu(bpetha)₂(H₂O)₂]}·2PF₆·3THF·2H₂O (4), {[Cu(bpetha)₂(H₂O)₂]}·2PF₆·3dioxane (5), and {[Cu(bpetha)₂(H₂O)₂]}·2PF₆·2-PrOH·2H₂O (6), containing 1-D Cu^{II}–bpetha double chains (Scheme 1). The formation of guest-binding hosts, detailed comparison of their crystal structures, guest selectivity, and guest-exchange properties will be discussed.

Experimental Section

Materials. All chemicals and solvents used during synthesis were reagent grade.

Synthesis of {[Cu(bpetha)₂(acetone)₂]}·2PF₆ (1). Single crystals suitable for X-ray analysis were prepared by careful diffusion of an acetone solution of bpetha (0.50 mmol) into an aqueous solution containing Cu(BF₄)₂·6H₂O (0.25 mmol) and NH₄PF₆ (0.75 mmol) in a straight glass tube. After a few days, purple crystals were obtained. Anal. Calcd for C₂₇H₃₀CuF₁₂N₄O₁P₂ {[Cu(bpetha)₂(acetone)]·2PF₆}: C, 41.57; H, 3.88; N, 7.06. Found: C, 41.57; H, 3.88; N, 7.18. IR (KBr pellet, cm⁻¹): 1700 w, 1620 m, 1560 w, 1508 w, 1431 m, 1230 w, 1068 m, 1032 m, 940 w, 845 s, 739 w, 603 w, 558 m, 533 m.

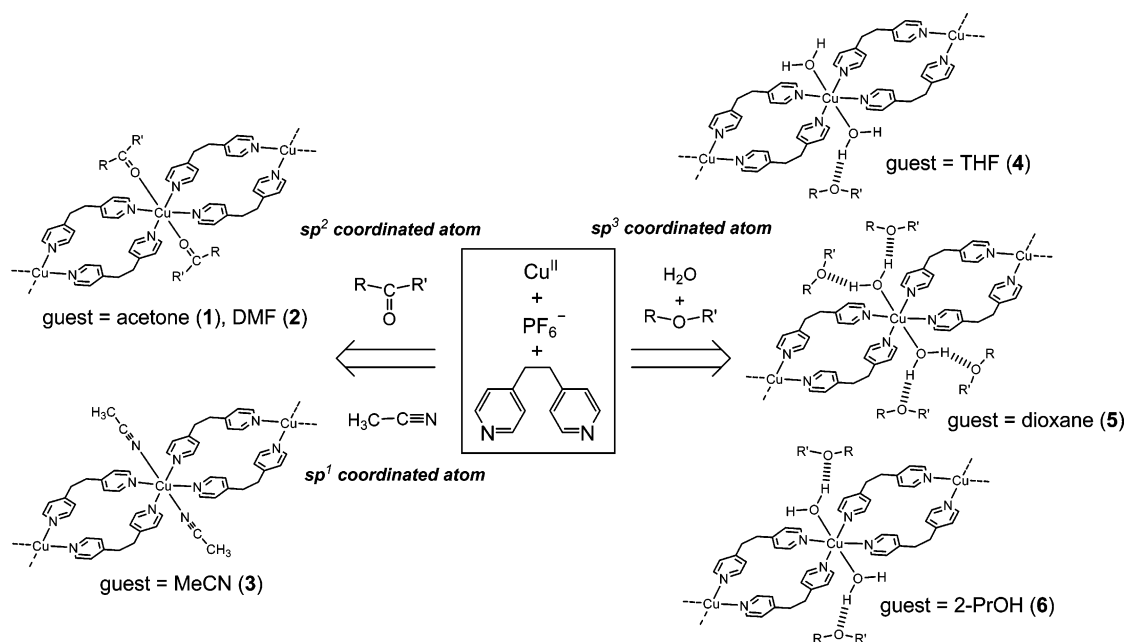
Synthesis of {[Cu(bpetha)₂(DMF)₂]}·2PF₆ (2). Single crystals suitable for X-ray analysis were prepared by careful diffusion of a DMF solution of bpetha (0.50 mmol) into an aqueous solution containing Cu(BF₄)₂·6H₂O (0.25 mmol) and NH₄PF₆ (0.75 mmol) in a straight glass tube. After a few days, sky-blue crystals were obtained. Anal. Calcd for C₃₀H₃₈CuF₁₂N₆O₂P₂: C, 41.51; H, 4.41; N, 9.86. Found: C, 41.65; H, 4.35; N, 9.69. IR (KBr pellet, cm⁻¹): 3079 w, 2934 w, 2871 w, 1656 s, 1619 s, 1560 m, 1505 w, 1431 m, 1414 m, 1391 m, 1250 w, 1227 w, 1211 w, 1193 w, 1099 m, 1070 m, 1031 m, 943 w, 876 s, 842 s, 662 m, 602 w, 558 s, 532 m.

Synthesis of {[Cu(bpetha)₂(MeCN)₂]}·2PF₆·2MeCN (3). Single crystals suitable for X-ray analysis were prepared by careful

- (3) (a) Kitaura, R.; Fujimoto, K.; Noro, S.; Kondo, M.; Kitagawa, S. *Angew. Chem., Int. Ed.* **2002**, *41*, 133–135. (b) Uemura, K.; Kitagawa, S.; Kondo, M.; Fukui, K.; Kitaura, R.; Chang, H.-C.; Mizutani, T. *Chem.—Eur. J.* **2002**, *8*, 3587–3600. (c) Matsuda, R.; Kitaura, R.; Kitagawa, S.; Kubota, Y.; Belosludov, R. V.; Kobayashi, T. C.; Sakamoto, H.; Chiba, T.; Takata, M.; Kawazoe, Y.; Mita, Y. *Nature (London)* **2005**, *436*, 238–241. (d) Yaghi, O. M.; Li, G.; Li, H. *Nature (London)* **1995**, *378*, 703–706.
- (4) Kitagawa, S.; Noro, S.; Nakamura, T. *Chem. Commun.* **2006**, 701–707.
- (5) (a) Beauvais, L. G.; Shores, M. P.; Long, J. R. *J. Am. Chem. Soc.* **2000**, *122*, 2763–2772. (b) Lefebvre, J.; Batchelor, R. J.; Leznoff, D. B. *J. Am. Chem. Soc.* **2004**, *126*, 16117–16125.
- (6) (a) Sharma, A. C.; Borovik, A. S. *J. Am. Chem. Soc.* **2000**, *122*, 8946–8955. (b) Ozin, G. A.; Gil, C. *Chem. Rev.* **1989**, *89*, 1749–1764.
- (7) (a) Reineke, T. M.; Eddaoudi, M.; Fehr, M.; Kelley, D.; Yaghi, O. M. *J. Am. Chem. Soc.* **1999**, *121*, 1651–1657. (b) Reineke, T. M.; Eddaoudi, M.; O'Keeffe, M.; Yaghi, O. M. *Angew. Chem., Int. Ed. Engl.* **1999**, *38*, 2590–2593. (c) Pan, L.; Adams, K. M.; Hernandez, H. E.; Wang, X.; Zheng, C.; Hattori, Y.; Kaneko, K. *J. Am. Chem. Soc.* **2003**, *125*, 3062–3067.

- (8) (a) Yaghi, O. M.; Davis, C. E.; Li, G.; Li, H. *J. Am. Chem. Soc.* **1997**, *119*, 2861–2868. (b) Li, H.; Davis, C. E.; Groy, T. L.; Kelley, D. G.; Yaghi, O. M. *J. Am. Chem. Soc.* **1998**, *120*, 2186–2187. (c) Chen, B.; Eddaoudi, M.; Reineke, T. M.; Kampf, J. W.; O'Keeffe, M.; Yaghi, O. M. *J. Am. Chem. Soc.* **2000**, *122*, 1155–11560.
- (9) (a) Noro, S.; Kitagawa, S.; Yamashita, M.; Wada, T. *Chem. Commun.* **2002**, 222–223. (b) Kitaura, R.; Onoyama, G.; Sakamoto, H.; Matsuda, R.; Noro, S.; Kitagawa, S. *Angew. Chem., Int. Ed.* **2004**, *43*, 2684–2687. (c) Maji, T. K.; Ohba, M.; Kitagawa, S. *Inorg. Chem.* **2005**, *44*, 9225–9231.
- (10) (a) Chen, B.; Fronczek, F. R.; Maverick, A. W. *Inorg. Chem.* **2004**, *43*, 8209–8211. (b) Chui, S. S.-Y.; Lo, S. M.-F.; Charmant, J. P. H.; Orpen, A. G.; Williams, I. D. *Science* **1999**, *283*, 1148–1150.

Scheme 1



Direct coordinations to Cu^{II} UMCs

diffusion of a MeCN solution of bptha (0.50 mmol) into an aqueous solution containing $\text{Cu}(\text{BF}_4)_2 \cdot 6\text{H}_2\text{O}$ (0.25 mmol) and NH_4PF_6 (1.00 mmol) in a straight glass tube. After a few days, blue crystals were obtained. Anal. Calcd for $\text{C}_{27}\text{H}_{31.5}\text{CuF}_{12}\text{N}_{5.5}\text{O}_{1.5}\text{P}_2$ ($\{[\text{Cu}(\text{bptha})_2] \cdot 2\text{PF}_6 \cdot 1.5\text{MeCN} \cdot 1.5\text{H}_2\text{O}\}_n$): C, 40.01; H, 3.92; N, 9.50. Found: C, 40.13; H, 3.93; N, 9.47. IR (KBr pellet, cm^{-1}): 2267 w, 1621 m, 1561 w, 1505 w, 1448 w, 1432 m, 1373 w, 1229 w, 1210 m, 1190 w, 1068 m, 1032 m, 940 w, 844 s, 740 w, 606 w, 557 m, 534 m.

Synthesis of $\{[\text{Cu}(\text{bptha})_2(\text{H}_2\text{O})_2] \cdot 2\text{PF}_6 \cdot 3\text{THF} \cdot 2\text{H}_2\text{O}\}_n$ (4). Single crystals suitable for X-ray analysis were prepared by careful diffusion of a THF solution of bptha (0.50 mmol) into an aqueous solution containing $\text{Cu}(\text{BF}_4)_2 \cdot 6\text{H}_2\text{O}$ (0.25 mmol) and NH_4PF_6 (0.75 mmol) in a straight glass tube. After a few days, purple crystals were obtained. Anal. Calcd for $\text{C}_{24}\text{H}_{26}\text{CuF}_{12}\text{N}_4\text{O}_1\text{P}_2$ ($\{[\text{Cu}(\text{bptha})_2(\text{H}_2\text{O})] \cdot 2\text{PF}_6\}_n$): C, 38.96; H, 3.54; N, 7.57. Found: C, 38.87; H, 3.54; N, 7.57. IR (KBr pellet, cm^{-1}): 1661 m, 1618 s, 1560 w, 1507 w, 1433 m, 1231 w, 1083 m, 1070 m, 1031 m, 845 s, 739 w, 598 w, 558 m.

Synthesis of $\{[\text{Cu}(\text{bptha})_2(\text{H}_2\text{O})_2] \cdot 2\text{PF}_6 \cdot 3\text{dioxane}\}_n$ (5). Single crystals suitable for X-ray analysis were prepared by careful diffusion of a dioxane solution of bptha (0.50 mmol) and an aqueous solution containing $\text{Cu}(\text{BF}_4)_2 \cdot 6\text{H}_2\text{O}$ (0.25 mmol) and NH_4PF_6 (0.75 mmol) in a Y-shaped glass tube. After a few days, blue crystals were obtained. Anal. Calcd for $\text{C}_{27.2}\text{H}_{31.4}\text{CuF}_{12}\text{N}_4\text{O}_{2.1}\text{P}_2$ ($\{[\text{Cu}(\text{bptha})_2(\text{H}_2\text{O})_{0.5}] \cdot 2\text{PF}_6 \cdot 0.8\text{dioxane}\}_n$): C, 40.76; H, 3.95; N, 6.99. Found: C, 40.51; H, 3.81; N, 6.95. IR (KBr pellet, cm^{-1}): 1619 m, 1561 w, 1507 w, 1431 m, 1230 w, 1068 w, 1032 w, 846 s, 558 m, 532 w.

Synthesis of $\{[\text{Cu}(\text{bptha})_2(\text{H}_2\text{O})_2] \cdot 2\text{PF}_6 \cdot 2\text{-PrOH} \cdot 2\text{H}_2\text{O}\}_n$ (6). Single crystals suitable for X-ray analysis were prepared by careful diffusion of a 2-PrOH solution of bptha (0.50 mmol) into an aqueous solution containing $\text{Cu}(\text{BF}_4)_2 \cdot 6\text{H}_2\text{O}$ (0.25 mmol) and NH_4PF_6 (1.00 mmol) in a straight glass tube. After a few days, blue crystals were obtained. Anal. Calcd for $\text{C}_{24.3}\text{H}_{32.2}\text{CuF}_{12}\text{N}_4\text{O}_{3.8}\text{P}_2$ ($\{[\text{Cu}(\text{bptha})_2(\text{H}_2\text{O})_2] \cdot 2\text{PF}_6 \cdot 0.1(2\text{-PrOH}) \cdot 1.7\text{H}_2\text{O}\}_n$): C, 36.73; H, 4.08; N, 7.05. Found: C, 36.77; H, 4.17; N, 7.15. IR (KBr pellet,

Hydrogen bonds via H_2O molecules

cm^{-1}): 1621 s, 1562 w, 1506 w, 1432 m, 1229 w, 1069 m, 1032 m, 842 s, 740 w, 606 w, 558 s.

Physical Techniques. Elemental analysis (C, H, N) was performed on a Perkin-Elmer Model 240C elemental analyzer. IR spectra ($400\text{--}4000\text{ cm}^{-1}$) were recorded on a Perkin-Elmer Spectrum 2000 spectrometer with samples prepared as KBr pellets. XRD data were collected on a Rigaku RINT-Ultima III using $\text{Cu K}\alpha$ radiation. Thermogravimetric analysis (TGA) was performed on a Rigaku Thermo Plus 2/TG8120 over the temperature range $25\text{--}500\text{ }^\circ\text{C}$ in a N_2 atmosphere. NMR experiments were carried out on a JEOL JNM-LA300WB spectrometer operating at a resonance frequency of 121.5 MHz for ^{31}P at room temperature. A 7 mm double-resonance magic-angle spinning (MAS) probe was used at a spinning speed ranging 4.0–4.3 kHz. The spectra were obtained by single pulse 90° irradiation (pulse length 5.7 μs) with proton decoupling. The X-ray photoelectron spectroscopy (XPS) measurements were carried out on a JEOL JPS-9200 spectrometer equipped with an Al $\text{K}\alpha$ X-ray source (1486.6 eV). Measurements were done in the 10^{-5} Pa range. Sample were powdered and spread on conductive, adhesive carbon tape fixed on the glass substrate. Generally, the C 1s binding energy (284.4 eV) due to hydrocarbon contamination from the diffusion pump is used to calibrate the binding energy. However, the weak C 1s peak of the hydrocarbon contamination was covered by the strong C 1s peak of the carbon tape. Therefore, we could not calibrate the binding energy. The obtained peaks were deconvoluted by double Gaussian. The adsorption isotherm measurement for N_2 gas was carried out at $-195\text{ }^\circ\text{C}$ by using an automatic volumetric adsorption apparatus (Autosorb-1; Quantachrome Instruments). A known weight (49.11 mg) of **1** was placed in the quartz tube; then, prior to measurements, the sample was dried under high vacuum at $70\text{ }^\circ\text{C}$ for 12 h to remove the solvated acetone molecules. The adsorbate was placed into the sample tube; then, the change in pressure was monitored and the degree of adsorption was determined by the decrease in the pressure at the equilibrium state.

Crystal Structure Determination. For compounds **2**, **4**, and **5**, data collections were carried out on a Rigaku R-Axis CS imaging

Table 1. Crystallographic Data for $\{[\text{Cu}(\text{bpetha})_2(\text{acetone})_2] \cdot 2\text{PF}_6\}_n$ (**1**), $\{[\text{Cu}(\text{bpetha})_2(\text{DMF})_2] \cdot 2\text{PF}_6\}_n$ (**2**), $\{[\text{Cu}(\text{bpetha})_2(\text{MeCN})_2] \cdot 2\text{PF}_6 \cdot 2\text{MeCN}\}_n$ (**3**), $\{[\text{Cu}(\text{bpetha})_2(\text{H}_2\text{O})_2] \cdot 2\text{PF}_6 \cdot 3\text{THF} \cdot 2\text{H}_2\text{O}\}_n$ (**4**), $\{[\text{Cu}(\text{bpetha})_2(\text{H}_2\text{O})_2] \cdot 2\text{PF}_6 \cdot 3\text{dioxane}\}_n$ (**5**), and $\{[\text{Cu}(\text{bpetha})_2(\text{H}_2\text{O})_2] \cdot 2\text{PF}_6 \cdot 2\text{-PrOH} \cdot 2\text{H}_2\text{O}\}_n$ (**6**)

	1	2	3	4	5	6
formula	$\text{C}_{30}\text{H}_{36}\text{N}_4\text{CuF}_{12}\text{O}_2\text{P}_2$	$\text{C}_{30}\text{H}_{38}\text{N}_6\text{CuF}_{12}\text{O}_2\text{P}_2$	$\text{C}_{32}\text{H}_{36}\text{CuF}_{12}\text{N}_8\text{P}_2$	$\text{C}_{36}\text{H}_{56}\text{N}_4\text{CuF}_{12}\text{O}_7\text{P}_2$	$\text{C}_{36}\text{H}_{52}\text{CuF}_{12}\text{N}_4\text{O}_8\text{P}_2$	$\text{C}_{27}\text{H}_{39}\text{CuF}_{12}\text{N}_4\text{O}_5\text{P}_2$
fw	838.11	868.14	886.16	1010.34	1022.30	853.10
crystal system	orthorhombic	monoclinic	orthorhombic	monoclinic	monoclinic	orthorhombic
<i>a</i> , Å	24.091(1)	26.852(2)	20.089(7)	28.556(2)	11.2924(5)	9.3168(16)
<i>b</i> , Å	34.462(2)	9.4757(5)	41.009(12)	9.5987(7)	9.1456(2)	23.612(5)
<i>c</i> , Å	9.0650(5)	20.534(2)	9.399(3)	16.9060(9)	22.5267(8)	16.710(5)
β , deg		133.273(2)		107.974(3)	103.6912(8)	
<i>V</i> , Å ³	7526.0(7)	3804.1(5)	7743.2(42)	4407.8(5)	2260.4(1)	3676.0(14)
space group	<i>Fddd</i> (No. 70)	<i>C2/c</i> (No. 15)	<i>Fdd2</i> (No. 43)	<i>Cc</i> (No. 9)	<i>P2/c</i> (No. 13)	<i>Pbcm</i> (No. 57)
<i>Z</i>	8	4	8	4	2	4
ρ (calcd) g cm ⁻³	1.479	1.516	1.520	1.522	1.502	1.541
<i>F</i> (000)	3416.00	1772.00	3608.00	2092.00	1054.00	1744.00
μ (Mo K α), cm ⁻¹	7.58	7.54	7.40	6.69	6.55	7.83
diffractometer	RAXIS-RAPID	RAXIS-CS	RAXIS-RAPID	RAXIS-CS	RAXIS-CS	RAXIS-RAPID
radiation (λ , Å)	0.71073	0.71073	0.71073	0.71073	0.71073	0.71073
temp, °C	-40	25	-170	-170	-170	-170
GOF	1.900	1.271	1.064	2.279	2.036	0.751
<i>R</i> ^a	0.0646	0.0871	0.0290	0.1137	0.0583	0.0628
<i>R</i> _w ^b	0.0927	0.1783	0.0546	0.2281	0.1828	0.1335
no. of observations	2013	3819	3878	4327	4534	2488
no. of variables	118	276	268	596	285	263

$$^a R = \sum ||F_o| - |F_c|| / \sum |F_o|. \quad ^b R_w = [\sum w(|F_o| - |F_c|)^2 / \sum w F_o^2]^{1/2}.$$

plate diffractometer with graphite monochromated Mo K α radiation. For compounds **1**, **3**, and **6**, data collections were carried out on a Rigaku R-AXIS RAPID imaging plate diffractometer with graphite-monochromated Mo K α radiation. The structures were solved by the direct methods SIR92¹¹ (**1**), SIR97¹² (**2**, **5**), SIR2002¹³ (**3**, **6**), and SHELX97¹⁴ (**4**) and expanded using Fourier techniques.¹⁵ The non-hydrogen atoms were refined anisotropically except for **4**. In **4**, the THF molecule interacting with the coordination-free H₂O molecule is refined isotropically, and the free THF one is fixed because of loose packing. Therefore, the result of the refinements of **4** is not good compared with other compounds. Hydrogen atoms of **1**, **2**, and **5** were included but not refined. Hydrogen atoms of **3**, **4**, and **6** were refined using the riding model. The refinements were carried out using full-matrix least squares techniques on *F*². All calculations were performed using the teXsan crystallographic software package¹⁶ (Molecular Structure Corporation) for **1**, **2**, and **5**, and the CrystalStructure crystallographic software package¹⁷ for **3**, **4**, and **6**. Crystal data and details of the structure determinations are summarized in Table 1.

Crystallographic data for structures reported in this paper have been deposited at the Cambridge Data Centre as supplementary

publication nos. CCDC-279536 (**1**), 279537 (**2**), 285765 (**3**), 279538 (**4**), 279539 (**5**), and 285766 (**6**). Copies of the data can be obtained free of charge on application to CCDC, 12 Union Road, Cambridge CB21EZ, U.K. (Fax: (+44) 1223-336-033. E-mail: deposit@ccdc.cam.ac.uk).

Results and Discussion

To obtain coordination polymers capable of binding several guest molecules at Cu^{II} axial sites, we utilized a Cu^{II}-bpetha-PF₆⁻ system as the main framework structure. It is well-known that the bpetha ligand with its flexible -CH₂-CH₂- spacer can form a 1-D double chain motif as shown in Scheme 1.¹⁸ Therefore, it is expected that assemblies of this 1-D motif have the structural flexibility, due to the absence of recognizable interactions between these double chains, to accommodate several guests. The PF₆⁻ anion with its weak coordination ability was employed as the counter-anion for the cationic 1-D [Cu(bpetha)₂]_n double chain to prevent the coordination of anions to Cu^{II} axial sites. As expected, the chain-assembling framework accommodates several guests by its flexibility (vide infra).

The basic coordination frameworks of **1**-**6** are similar. An ORTEP view with its numbering scheme around a Cu^{II} center of **1** is shown in Figure 1a. The Cu^{II} ion has an elongated octahedral environment with four bpetha nitrogen atoms in the equatorial plane and two oxygen atoms of acetone molecules at the axial sites. In **1**, the Cu-O bond distance (2.497(4) Å) is considerably longer than the Cu-N bond distances (2.010(3) Å), indicative of a Jahn-Teller

- (11) SIR92: Altomare, A.; Burla, M. C.; Carnalli, M.; Cascarano, M.; Giacovazzo, C.; Guagliardi, A.; Polidori, G. *J. Appl. Crystallogr.* **1994**, *27*, 435.
- (12) SIR97: Altomare, A.; Burla, M. C.; Carnalli, M.; Cascarano, G. L.; Giacovazzo, C.; Guagliardi, A.; Moliterni, A. G. G.; Polidori, G.; Spagna, R. *J. Appl. Crystallogr.* **1999**, *32*, 115-119.
- (13) SIR2002: Burla, M. C.; Camalli, M.; Carrozzini, B.; Cascarano, G. L.; Giacovazzo, C.; Polidori, G.; Spagna, R. *J. Appl. Crystallogr.* **2003**, *36*, 1103.
- (14) Sheldrick, G. M. SHELX-97: Program for Crystal Structure Determination. University of Göttingen, Germany, 1997.
- (15) DIRDIF94: Beurskens, P. T.; Admiraal, G.; Beurskens, G.; Bosman, W. P.; de Gelder, R.; Israel, R.; J. Smits, M. M. The DIRDIF-94 program system, Technical Report of the Crystallography Laboratory, University of Nijmegen, The Netherlands, 1994.
- (16) teXsan: Crystal Structure Analysis Package. Molecular Structure Corporation, 1985 and 1999.
- (17) CrystalStructure 3.7.0: Crystal Structure Analysis Package. Rigaku and Rigaku/MS: The Woodlands, TX, 2000-2005.

- (18) (a) Kondo, M.; Shimamura, M.; Noro, S.; Kimura, Y.; Uemura, K.; Kitagawa, S. *J. Solid State Chem.* **2000**, *152*, 113-119. (b) Hernández, M. L.; Barandika, M. G.; Urriaga, M. K.; Cortés, R.; Lezama, L.; Arriortua, M. I.; Rojo, T. *J. Chem. Soc., Dalton Trans.* **1999**, 1401-1406.

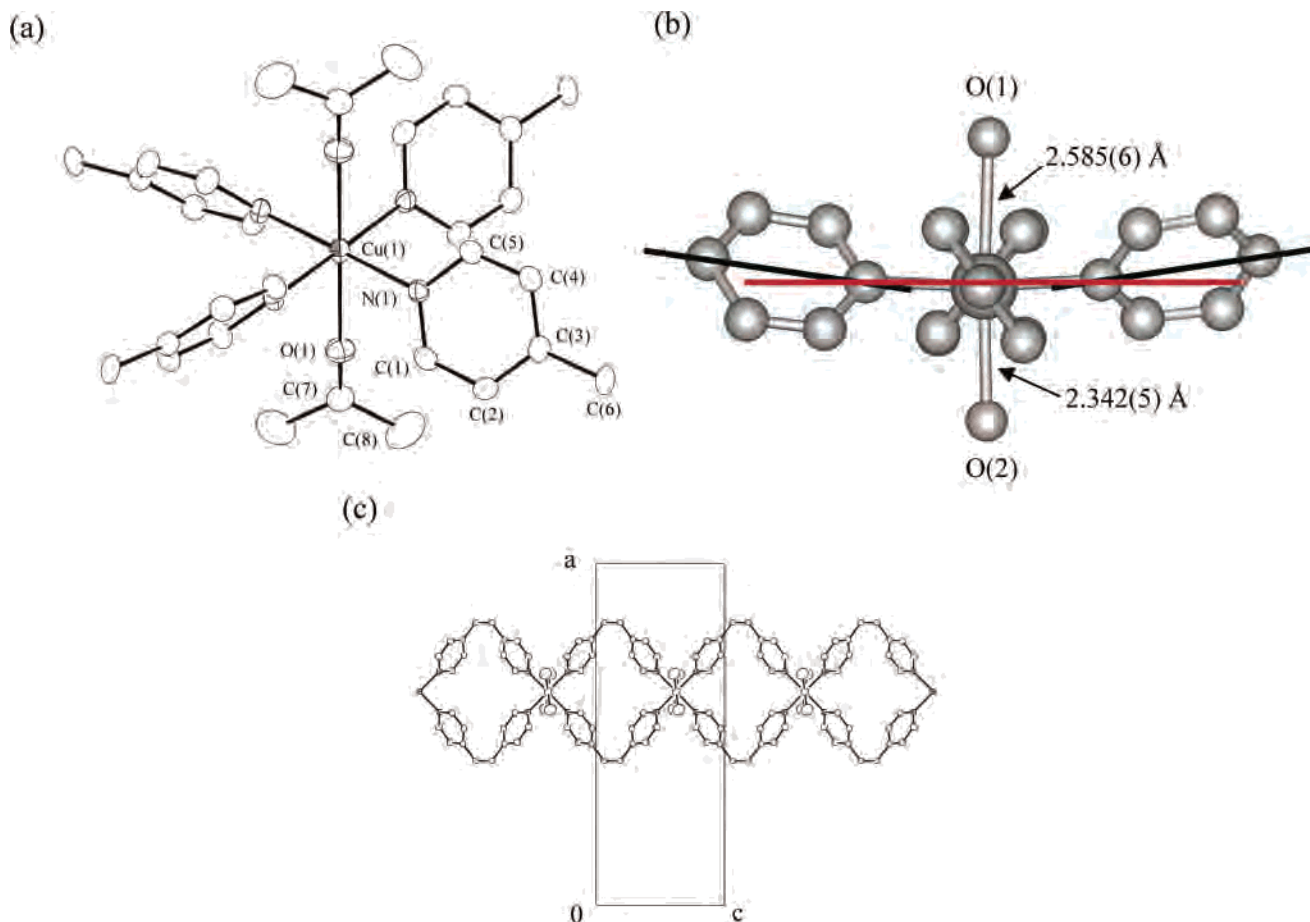


Figure 1. (a) ORTEP view (30% probability) of a Cu^{II} center of **1**. (b) View of a distorted Cu^{II} center of **4**. (c) ORTEP view (30% probability) of a 1-D chain running along the *c*-axis of **1**. The hydrogen atoms are omitted for clarity.

effect. In compounds **2–6**, DMF (2.515(5) Å (**2**)), MeCN (2.439(2) Å (**3**)), and H₂O (2.333(7) and 2.591(9) Å for **4**, 2.375(3) Å for **5**, and 2.451(3) Å for **6**) molecules are coordinated to the axial sites of Cu^{II} centers. The axial bonds in **4** are asymmetric. As shown in Figure 1b, two pyridine rings in this compound are tilted slightly toward one axial site, and this may hinder approach of the H₂O(1) molecule to the Cu^{II} center, resulting in a weak Cu–O(1) bond (2.591(9) Å). In contrast, the H₂O(2) molecule approaches much closer to the Cu^{II} center, forming a shorter Cu–O(2) bond (2.333(7) Å) than any of the other Cu–O(H₂O) bonds in compounds **4–6**. As H₂O is a small Lewis base guest, this result indicates that coordination of the pyridine groups of the bpeha ligands strongly influences the approach of Lewis base guests to the Cu^{II} axial sites. The bpeha ligand is capable of adopting either gauche or anti conformations and can therefore act as either an angular or a linear spacer ligand, respectively.¹⁹ In **1–6**, all bpeha ligands were in the anti form. Each bpeha ligand bridges Cu^{II} ions to form a 1-D double chain, as illustrated in Figure 1c. The intrachain Cu···Cu distances in **1–6** are in the range 9.07–9.60 Å. Although this chain creates a small grid with dimensions of ca. 2.4 × 2.1 Å (Figure 2),²⁰ the displaced stacks of 1-D

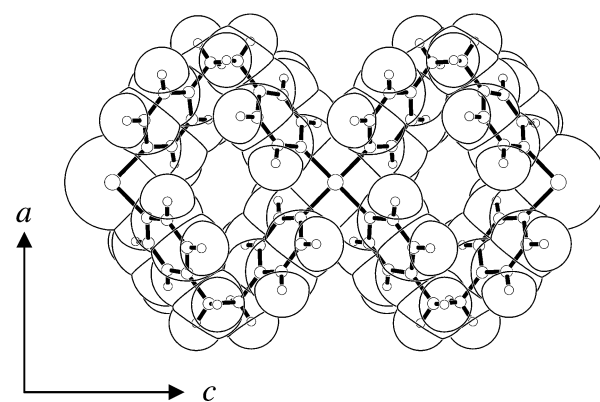


Figure 2. Microporous space within the 1-D double chain of **1** along the *b*-axis.

chains contain no 1-D channels. In **1**, the 1-D chains assemble without any notable interchain interactions to form 2-D layers with intercalated PF₆[−] anions and guest acetone molecules, as shown in Figure 3. The acetone guests are directly bound at the Cu^{II} axial sites via coordination bonds; there is no coordinative interaction between the host network and the PF₆[−] anions. The following section contains a detailed structural comparison of **1–6**.

It should be emphasized that the assembly of 1-D [Cu-(bpeha)₂]_{*n*} double chains is flexible. A view of the layers constructed from these chains is presented in Figure 4. The flexibility of the –CH₂–CH₂– moiety between aromatic

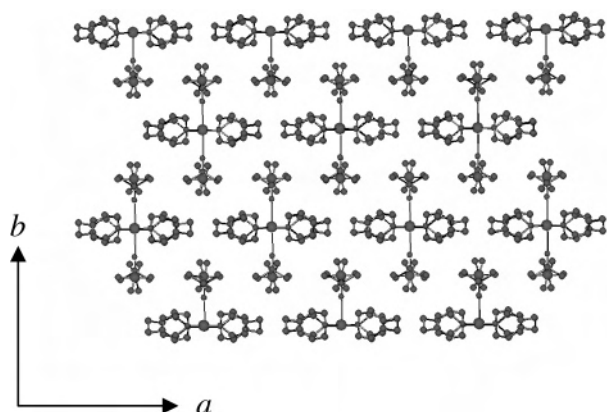
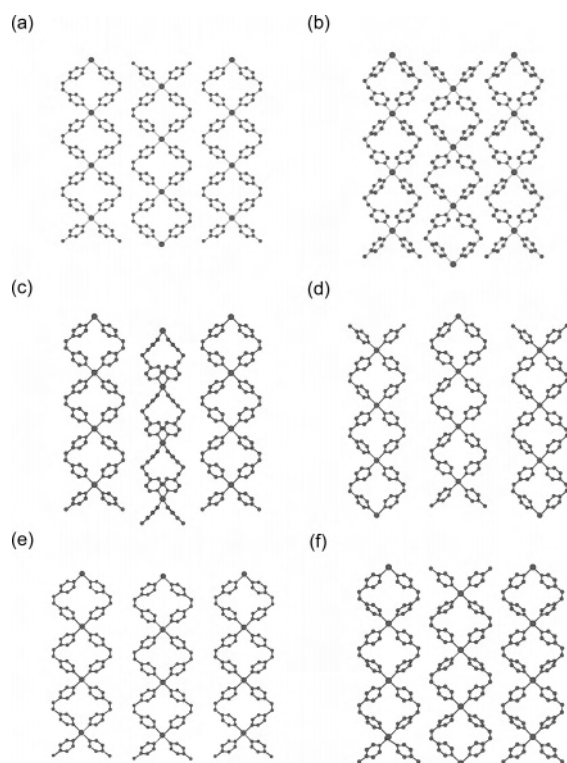
(19) Hennigar, T. L.; MacQuarrie, D. C.; Losier, P.; Rogers, R. D.; Zaworotko, M. J. *Angew. Chem., Int. Ed. Engl.* **1997**, *36*, 972–973.

(20) The size was measured by considering van der Waals radii for constituting atoms.

Table 2. Characteristic Distances (Å) and Guest-Accessible Void Space (%) of **1–6**

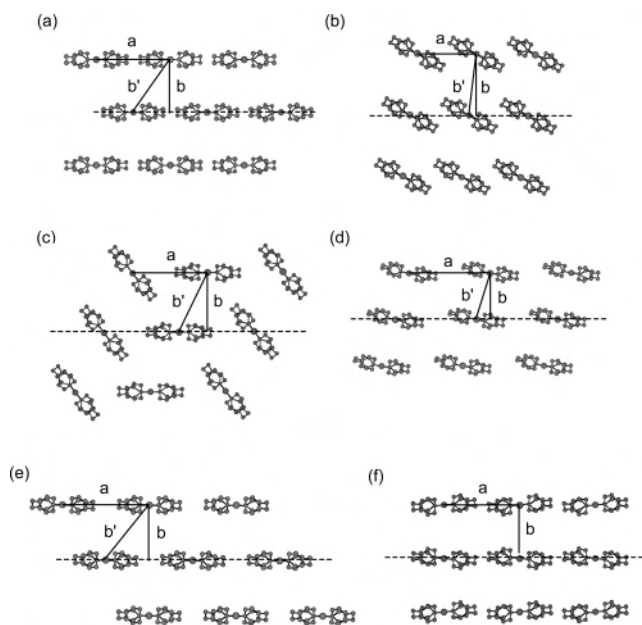
		1	2	3	4	5	6
guests		acetone	DMF	MeCN	H ₂ O, THF	H ₂ O, dioxane	H ₂ O, 2-PrOH
intrachain Cu ^{II} –Cu distance		9.07	9.48	9.40	9.60	9.15	9.32
Cu ^{II} –(axial guest) distance		2.497(4)	2.515(5)	2.439(2)	2.333(7), 2.591(9)	2.375(3)	2.451(3)
interchain distance	<i>a</i>	12.0	9.8	11.4	14.2	13.9	11.8
interlayer distance	<i>b</i>	8.6	10.2	9.0	8.1	7.3	8.3
	<i>b'</i>	11.7	10.3	9.9	8.5	11.4	
guest-accessible void space		28.2	24.6	25.5	39.1	39.0	27.1

pyridines in the bpetha ligand allows for the regulation of the intrachain Cu^{II}–Cu^{II} distances, as shown in Table 2. The layers in **1–6** are classified into three types on the basis of the mutual relationships of neighboring chains. **5** has a layer in which all the chains have matching phases. (phase here is defined as the intrachain Cu–Cu period.) In **3**, the chains

**Figure 3.** View of the alternate stack of the [Cu(bpetha)₂]_n layers and PF₆[−]/acetone ones of **1** along the *c*-axis. The hydrogen atoms are omitted for clarity.**Figure 4.** Comparison of the 2-D layers constructed from the 1-D [Cu(bpetha)₂]_n double chains in (a) **1**, (b) **2**, (c) **3**, (d) **4**, (e) **5**, and (f) **6**. Axially-coordinated guests and the hydrogen atoms are omitted for clarity.

are slightly shifted with respect to each other. Other coordination polymers form a layer in which the phase of neighboring chains is shifted by a half-period. In addition, the 1-D chains of **2**, **4**, and **6** tend to align along the plane constructed of connected Cu^{II} ions within a layer, as shown in Figure 5, in sharp contrast to their orientation in **1** and **5**. In **3**, the 1-D chains are alternately aligned parallel to and at an angle to this plane. The stacking of the layers is also flexible, as illustrated in Figure 5. The neighboring layers of **1–5** are stacked out of alignment; in contrast, those of **6** are not shifted. These layers have considerable flexibility, with degrees of freedom defined by four factors: intrachain Cu^{II}–Cu^{II} distance, form of assembly within the layers, degree of chain tilting, and stacking form between the layers. Such flexibility is unique and useful for the adaptable capture of various guests.

Although no PF₆[−] counterions form coordination bonds with the Cu^{II} ions in any of these coordination polymers, some interact with H₂O. In **4**, one PF₆[−] anion interacts with both the coordinated and the free H₂O molecules via hydrogen bonds,²¹ and another binds solely to the free H₂O molecule, also through a hydrogen bond (2.75(2) Å). In **6**, the PF₆[−] anions form weak hydrogen bonds with free H₂O molecules (O[⋯]F = 3.093(8) and 3.103(9) Å).

**Figure 5.** Comparison of the stacking forms of the [Cu(bpetha)₂]_n layers in (a) **1**, (b) **2**, (c) **3**, (d) **4**, (e) **5**, and (f) **6**. Axially-coordinated guests, free guests, PF₆[−] anions, and the hydrogen atoms are omitted for clarity. The dashed lines indicate a plane constructed of connected Cu^{II} ions within a layer.

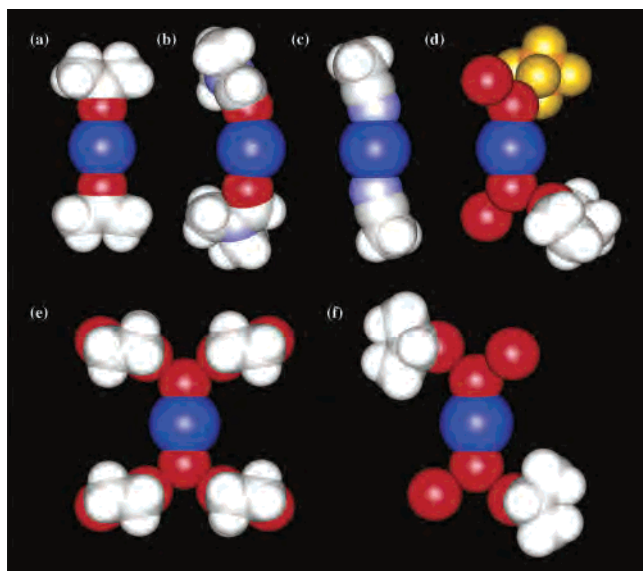


Figure 6. Comparison of the guest-binding forms around the Cu^{II} axial sites in (a) **1**, (b) **2**, (c) **3**, (d) **4**, (e) **5**, and (f) **6**. The coordinated pyridine groups of the bpetha ligands and the hydrogen atoms of the hydroxy groups are omitted for clarity (red, O; sky-blue, N; gray, C; white, H; blue, Cu; yellow, F; orange, P).

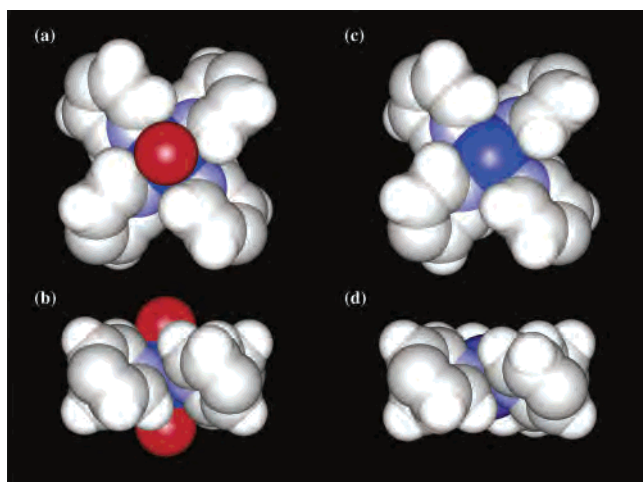


Figure 7. Corey–Pauling–Koltun (CPK) model around the Cu^{II} center (a and b) with and (c and d) without coordinated H₂O molecules in **4** (red, O; sky-blue, N; gray, C; white, H; blue, Cu). Figure 7(a) and (c) show the view parallel to the axial axis, and Figure 7(b) and (d) perpendicular to the axial one.

The 1-D [Cu(bpetha)₂]_n coordination polymers bind various guest molecules. Acetone, DMF, and MeCN guests of **1**, **2**, and **3**, respectively, are bound directly to the axial sites of Cu^{II} centers, as shown in Figure 6a–c. In **3**, other free MeCN guests are also included in vacant spaces. In contrast, the THF, dioxane, and 2-PrOH guests of **4**, **5**, and **6**, respectively, are captured not by coordination bonds but by other weak interactions. In **4**, there are three kinds of THF molecules: the first is bound by coordinated H₂O molecules via a hydrogen bond (O⋯O = 2.741(12) Å), as shown in Figure 6d; the second interacts weakly with the coordination-free H₂O molecules, also via a hydrogen bond (O⋯O = 3.09(2) Å); and the third is bonding-free. In addition to these THF guests, **4** incorporates free H₂O guests, forming hydrogen bonds. In **5**, both oxygen atoms of certain dioxane

Table 3. Donor Number (DN) of Guest Molecules

	DN
H ₂ O	18.0
acetone	17.0
DMF	26.6
MeCN	14.1
THF	20.0
dioxane	14.8
2-PrOH	>20.0

molecules interact with coordinated H₂O molecules via hydrogen bonds (2.704(4) and 2.711(4) Å), as illustrated in Figure 6e, and free dioxane molecules also exist in this crystal. Interestingly, the free dioxane guests are captured within the layers of 1-D [Cu(bpetha)₂]_n double chains. In **6**, the 2-PrOH guests interact with the coordinated H₂O molecules via hydrogen bonds (2.867(5) Å), as shown in Figure 6f. In addition, there are free H₂O guests also incorporated by hydrogen bonds. Here, H₂O molecules play an important role in the capture of Lewis base guest molecules. For guests with a carbonyl or cyano substituent, no H₂O molecules are included in the crystals and guests coordinated directly to Cu^{II} centers. However, in the presence of other guests (i.e., in **4**–**6**), the H₂O molecules coordinate to the Cu^{II} centers and act as hydrogen bonding sites for guest-binding (see Figure 6d–f). Therefore, one can regard the H₂O molecules both as small guests and as ligands supporting guest binding.

As mentioned above, the type of host–guest interaction is dependent on the nature of the guest molecule. The Lewis acid Cu^{II} ion generally interacts with Lewis base guest molecules through coordinative and electrostatic interactions (ion–ion and ion–dipole interactions). Because such electrostatic interactions between the cationic Cu^{II} centers and the neutral guests are weaker than coordinative ones, we consider only coordinative interactions in our discussion. Table 3 lists the donor number (DN) of guests used in this work (a molecule's DN is related to the strength of its coordination bonds),²² but information on guest selectivity could not be obtained from this parameter. Therefore, another factor, namely steric hindrance, is important in governing guest-binding selectivity in this Cu^{II}–bpetha system. Because steric hindrance does not allow the Cu^{II}-coordinated pyridine rings to be coplanar, the Cu^{II} axial sites have restricted space for attack by guests, as shown in Figure 7. In the case of guests with an sp³ oxygen atom bound to a methylene group, the ideal Cu–O–C angle is ca. 109.5°. However, steric hindrance between the pyridine rings of bpetha ligands and O-coordinated methylene groups of the guests causes the inclusion of coordination-free guests.²³ In contrast, guests with the sp² oxygen of a C=O group afford the ideal Cu–

(21) There are two crystallographically independent PF₆[−] anions in the crystal. The F atoms of one PF₆[−] anion are intricately disordered. Therefore, the hydrogen-bonding distances are not shown.

(22) (a) Gutmann, V. *The Donor–Acceptor Approach to Molecular Interactions*; Plenum Press: New York, 1978. (b) Linert, W.; Fukuda, Y.; Camard, A. *Coord. Chem. Rev.* **2001**, *218*, 113–152.

(23) Some coordination compounds with Cu^{II}-coordinated THF or 2-PrOH guests have been previously reported. THF: Chen, B.; Fronczek, F. R.; Maverick, A. W. *Inorg. Chem.* **2004**, *43*, 8209–8211. 2-PrOH: Yonemura, M.; Arimura, K.; Inoue, K.; Usuki, N.; Ohba, M.; Okawa, H. *Inorg. Chem.* **2003**, *41*, 582–589.

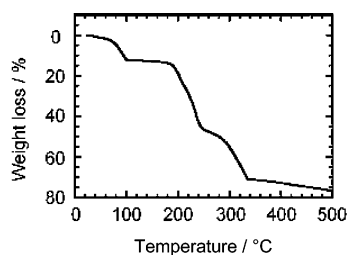


Figure 8. TGA curve of **1**.

O–C angle of ca. 120° ,²⁴ possibly weakening the steric hindrance to some extent, compared with that encountered with an sp^3 oxygen. In addition, acetone and DMF guests in **1** and **2**, respectively, coordinate to the Cu^{II} ions with less steric hindrance: the Cu–O–C bond angles (180° and $156.6(2)^\circ$, respectively) deviate considerably from the ideal value. The linear MeCN molecule with an sp nitrogen coordinates to the Cu^{II} center with the ideal Cu–N≡C bond angle of ca. 180° , thus experiencing little steric hindrance. Therefore, it is worth noting that the $\{[Cu(bpetha)_2] \cdot 2PF_6\}_n$ host can identify a variety of guest molecules by degrees of steric hindrance around coordinating atoms.

The observed Cu–N≡C bond angle in **3** is $162.65(16)^\circ$, as shown in Figure 6c. Upon detailed examination of the environment around the $-CH_3$ group of the coordinated MeCN, we found C⋯F distances of 3.157(3) and 3.161(3) Å between the $-CH_3$ group and neighboring PF_6^- anions. A MeCN molecule has a positive Mulliken charge on the $-CH_3$ group due to the presence of the electron-withdrawing $-C\equiv N$ group.²⁵ Therefore, the $-CH_3$ group of MeCN may be attracted to anionic PF_6^- anions through electrostatic interactions, leading to a deviation from the ideal bond angle.

The framework stability and guest-exchange properties in these guest-binding coordination polymers were investigated. Compounds **1** and **2** contain only the coordinated guests acetone and DMF in their respective frameworks. The XRD pattern of **2** with its DMF guests shows several sharp, intense peaks and is similar to that simulated from the results of the single crystal structural analysis, indicative of retention of the original assembly form. Partially desolvated **1** also affords a similar XRD pattern to its corresponding simulated pattern, again indicating that the partial removal of acetone causes no drastic structural change. In contrast, the XRD patterns of partially desolvated **3**, **4**, **5**, and **6** are considerably different from simulated results. In contrast to **1** and **2**, they have coordination-free guests, which are easily removed at room temperature and atmospheric pressure. Therefore, these results point out that coordination-free guest molecules play an important role in the assembly form of Cu–bpetha– PF_6^- systems.

Figure 8 shows the TGA curve of **1**, which loses its coordinated acetone molecules up to $100^\circ C$, resulting in a framework that is stable up to ca. $180^\circ C$. To examine the structure of **1** after complete removal of acetone, we

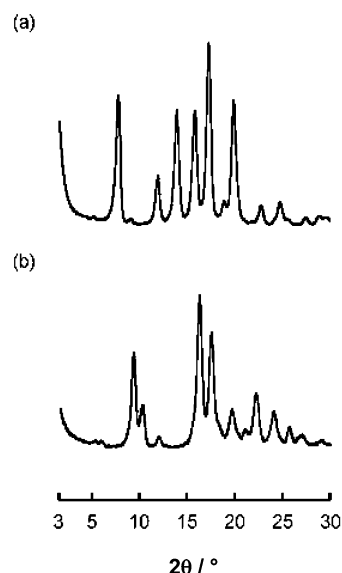


Figure 9. XRD patterns of **1** (a) with and (b) without acetone guests.

measured the XRD pattern after drying at $70^\circ C$ in a vacuum for 4 h. The complete removal of acetone guests was confirmed by TGA and by IR spectroscopy (see Supporting Information). Despite an alteration in the coordination environment around the Cu^{II} centers, the sample color scarcely changes. As shown in Figure 9, the XRD pattern of fully desolvated **1** has sharp diffraction peaks but is considerably different from that of **1** with acetone guests, indicative of retention of crystallinity and a change in crystal structure. However, when fully desolvated **1** is exposed to acetone vapor for 2 h, **1** is re-formed, indicating that the host framework $\{[Cu(bpetha)_2] \cdot 2PF_6\}_n$ reversibly binds acetone molecules at the Cu^{II} centers. Here, a question arises: how is the coordination environment around the Cu^{II} centers in **1** without acetone molecules? Two possibilities are considered: one is the formation of the coordinatively unsaturated Cu^{II} centers at the axial positions, and the other is an axial ligand exchange between acetone molecules and PF_6^- anions on the Cu^{II} centers during desolvation. Fujita and co-workers have recently found an axial-ligand-exchange process between H_2O molecules and NO_3^- anions on Co^{II} centers during desolvation, with keeping the main framework and the crystallinity.²⁶ Ordinarily, a PF_6^- anion has poor coordination ability for usual transition metal ions, hardly providing complexes with a direct bond between a metal atom and a fluorine atom. However, in the case of Cu^{II} complexes, which undergo Jahn–Teller distortion and give a (4+2) coordination environment, a PF_6^- anion could occupy the axial sites of the Cu^{II} ion. Indeed, we have reported the Cu^{II} –4,4′-bipyridine coordination polymers with coordinating PF_6^- anions.²⁷

To check the environment around the PF_6^- anions before and after the removal of the acetone molecules, we measured the solid-state ^{31}P NMR and XPS spectra. Figure 10 displays

(24) Korzeniak, T.; Stadnicka, K.; Rams, M.; Sieklucka, B. *Inorg. Chem.* **2004**, *43*, 4811–4813.

(25) The Mulliken charge was calculated by Gaussian03W software, using B3LYP/6-31G**.

(26) Takaoka, K.; Kawano, M.; Tominaga, M.; Fujita, M. *Angew. Chem., Int. Ed.* **2005**, *44*, 2151–2154.

(27) Noro, S.; Kitaura, R.; Kondo, M.; Kitagawa, S.; Ishii, T.; Matsuzaka, H.; Yamashita, M. *J. Am. Chem. Soc.* **2002**, *124*, 2568–2583.

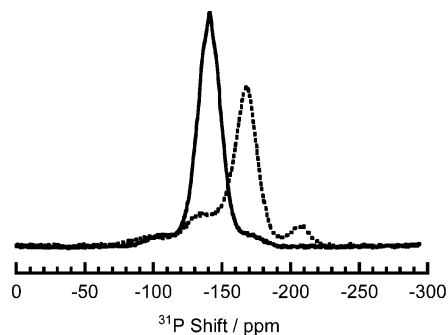


Figure 10. Solid-state ^{31}P -NMR spectra of **1** (solid line) and desolvated **1** (dotted line) at 25 °C.

the observed ^{31}P NMR spectra of **1** and desolvated **1** at 25 °C. Generally, the spectra of the PF_6^- anion have a septet pattern due to a spin–spin coupling of the ^{19}F nucleus ($I = 1/2$) with the ^{31}P nucleus. However, observed spectra show extremely broad signals, which is attributed to the effect of paramagnetic Cu^{II} ions ($\text{Cu}^{\text{II}}\cdots\text{P}$ distance in **1**: 6.27 Å). The chemical shift of **1** (−141.1 ppm) is close to one of a free PF_6^- anion (−143.6 ppm) in solution.²⁸ In contrast, the signal of the desolvated **1** is shifted upfield relative to that for **1**. Figure 11 shows the XPS spectra of the F 1s region. As shown in Figure 11a, the strong peak is observed for **1** at the binding energy of 689.6 eV, with the weak peak at the binding energy of 687.0 eV. After the removal of acetone guest molecules, the intensity of the peak at 687.0 eV in the desolvated **1** increases, as shown in Figure 11b. The spectral change observed in the ^{31}P NMR and XPS measurements is explained as follows. In **1**, there are free PF_6^- anions in the crystal, which was confirmed by the single-crystal X-ray diffraction measurement and the solid-state ^{31}P NMR spectra. Therefore, the strong peak at 689.6 eV in the XPS spectra of **1** (Figure 11a) corresponds to the free PF_6^- anions. After the removal of acetone guest molecules, the environment around the PF_6^- anions considerably changes. The upfield shift in the solid-state ^{31}P NMR spectra of the desolvated **1** is attributed to the paramagnetic shift.²⁹ In other words, it is expected that the PF_6^- anions approach the axial sites of the Cu^{II} centers after the removal of the acetone molecules. The peak at 687.0 eV in the desolvated **1** corresponds to the F atoms near the axial sites of the Cu^{II} centers. The weak peak at 687.0 eV in **1** is observed due to the fractional formation of the desolvated **1** under reduced pressure of $\sim 10^{-5}$ Pa. So, we conclude that the coordinatively unsaturated Cu^{II} axial sites formed by the removal of the acetone molecules are protected temporarily by the PF_6^- anions.

The result of N_2 adsorption and desorption isotherms in the desolvated **1** at −196 °C also supports the axial ligand exchange between acetone molecules and PF_6^- anions on the Cu^{II} centers during desolvation of **1**. The desolvated **1** shows type II isotherms (see Supporting Information), indicative of nonporous structure. Therefore, the crystalline

framework of the desolvated **1** has not enough space for guests to attack the axial sites of the Cu^{II} centers without a structural change.

Next, we investigated the guest-exchange properties of **1**. When **1** is exposed to MeCN vapor, a guest exchange from acetone to MeCN occurs, forming **3'**. In this process, the sample color changes from purple to sky-blue, indicating that the strength of the ligand field is altered as a consequence of this guest exchange.^{22b} The XRD pattern of **3'** is different from that calculated from the single-crystal structural data of **3**, indicating the formation of a new crystalline phase induced by the MeCN guest. The IR spectra of **3'** show the $\text{C}\equiv\text{N}$ stretching vibration of MeCN guests around 2270 cm^{-1} . This guest exchange is reversible: exposure of **3'** to acetone vapor reforms **1**. All guest-exchange phenomena were checked by XRD and IR measurements (see Supporting Information). Similar experiments were performed with $\text{H}_2\text{O}/\text{THF}$ vapor. When **1** is exposed to $\text{H}_2\text{O}/\text{THF}$ vapor, a guest exchange from acetone to $\text{H}_2\text{O}/\text{THF}$ occurs, forming **4'**. In this process, the sample color again changes from purple to sky-blue, indicative of an alteration in the coordination environment of Cu^{II} . However, the color of **4'** changes from sky-blue to bluish-purple immediately after the sample was brought out into the atmosphere. The IR spectra of the obtained bluish-purple sample **7** show no $\text{C}-\text{O}-\text{C}$ asymmetric stretching vibration of THF guests around 1100 cm^{-1} . This is probably due to the rapid removal of THF guests from the host framework. As shown in Figure 12a, the XRD pattern of **7** is different from that calculated from the single-crystal structural data of **4**, once again indicating the formation of a new crystalline phase induced by $\text{H}_2\text{O}/\text{THF}$ vapor. This guest exchange is also reversible: exposure of **7** to acetone vapor re-forms **1** (see Figure 12b). We also exposed **1** to H_2O vapor. The resulting sample has a similar color (bluish-purple) and XRD pattern to those of **7**. This result clearly indicates that **7** occupies only H_2O guests. This guest-exchange process is summarized in Scheme 2. The compound $\{[\text{Cu}(\text{bpetha})_2(\text{acetone})_2]\cdot 2\text{PF}_6\}_n$ (**1**) showed a discernible color change during the guest-exchange process. Such a solvatochromic effect is one of the unique functionalities of transition metal ions having dynamic coordination sites,^{5,9c} and the Cu^{II} ion is a good candidate for the creation of chromic sensors.

In general, porous coordination polymers with metal centers capable of binding guest molecules almost fully retain their original assembled topologies even upon coordination and removal of guests at the metal centers. In other words, the guest-accessible space around the metal centers remains almost unchanged. Therefore, they show not only substituent-but also size-selective uptake of guest molecules.^{8,9c} The $\{[\text{Cu}(\text{bpetha})_2]\cdot 2\text{PF}_6\}_n$ host reported here also recognizes the size and shape of introduced guests at the Cu^{II} centers having a restricted coordination space, achieving selective guest coordination. However, by flexibly changing its assembly form in response to the nature of the guest molecules, this host can even incorporate guests having no ability to approach the Cu^{II} centers. Therefore, it should be noted that the $\{[\text{Cu}(\text{bpetha})_2]\cdot 2\text{PF}_6\}_n$ host is a novel host–guest system

(28) Okubo, T.; Kitagawa, S.; Kondo, M.; Matsuzaka, H.; Ishii, T. *Angew. Chem., Int. Ed. Engl.* **1999**, *38*, 931–933.

(29) La Mar, G. N.; Horrocks, W. D., Jr.; Holm, R. H. *NMR of Paramagnetic Molecules: Principles and Applications*; Academic Press: New York, 1973.

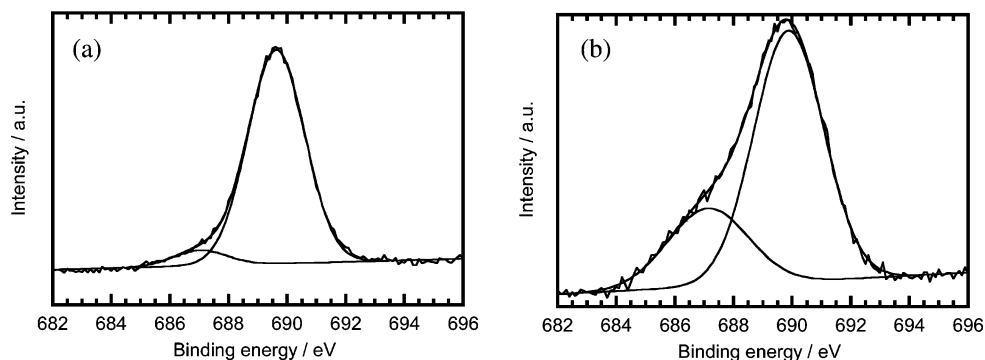


Figure 11. XPS spectra of F 1s region in (a) **1** and (b) desolvated **1** at 24 °C.

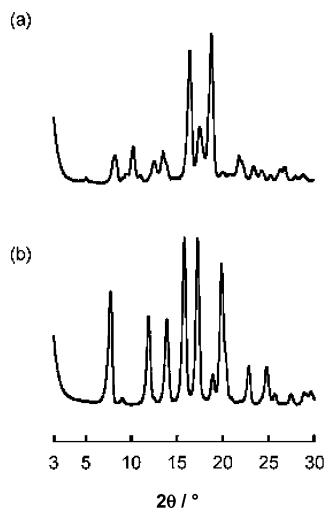
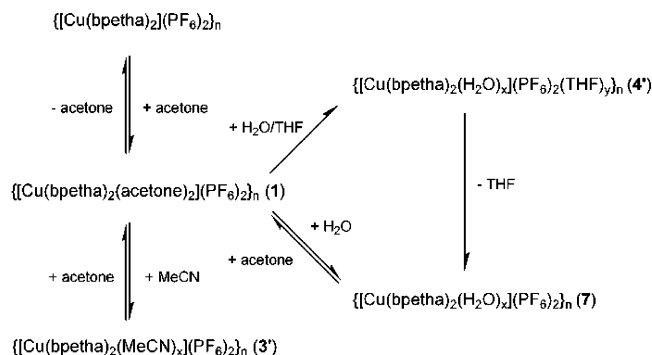


Figure 12. XRD patterns of (a) **7** (obtained by exposing **1** to H₂O/THF 1:1 vapor for 2 days and into the atmosphere) and (b) **7** exposed to acetone vapor for 3 h.

Scheme 2



that shows not only guest selectivity but also flexibility of assembly. This flexibility is clearly reflected in the guest-accessible void space of compounds **1–6** listed in Table 2.³⁰ This void space varies over the range of 24.6–39.1%. Such plasticity in the framework is attributed to fact that the 1-D [Cu(bpetha)₂]_n chains are assembled without strong interchain interactions, that is, involving only van der Waals interactions and weak electrostatic interactions with PF₆⁻ anions.

There are only a limited number of examples to date of host–guest systems based on a 1-D coordination motif,

compared with those based on 2-D or 3-D motifs. The crystalline host [Ni(SCN)₂(isoH)₂]_n (isoH = isonicotinic acid) forms a 1-D chain bridged by SCN⁻ anions.³¹ Neighboring 1-D chains assemble via hydrogen bonding interactions between the carboxylic acid groups of the isoH ligands, forming 2-D host layers, within which a variety of aromatic guests are incorporated by π–π interactions. [M₂(bza)₄(pyz)]_n (M = Rh^{II} and Cu^{II}; bza = benzoate; pyz = pyrazine) affords a 1-D coordination motif constructed from the lantern-like metal benzoate and a pyz bridge.³² Each 1-D coordination motif aggregates by π–π stacking of the aromatic rings of the ligands, forming 1-D channels. Several gases (O₂, N₂, CH₄, and CO₂) and EtOH vapor are incorporated into the 1-D channels. The zigzag 1-D coordination polymer [Cu(bhnq)]_n (H₂bhnq = 2,2'-bis(3-hydroxy-1,4-naphthoquinone)) incorporates EtOH, THF, and dioxane guests between its 1-D structures.³³ The π–π interaction between bhnq²⁻ ligands and the CH⋯O hydrogen bonding interactions acts to stabilize the assembled structures. Compared with the {[Cu(bpetha)₂]·2PF₆]_n system of this work, the three above-mentioned systems have in common effectual interactions such as hydrogen bonding and aromatic interactions operating between the 1-D coordination motifs. Therefore, they ought not to be called host–guest systems on the basis of simple 1-D coordination motifs. However, because the [Cu(bpetha)₂]_n chains do not assemble through any of the effectual interactions mentioned above, they can legitimately be regarded as a simple 1-D coordination motif that behaves as a clathrate-like solid. It should be emphasized that, to our knowledge, the {[Cu(bpetha)₂]·2PF₆]_n system is the first example to show a variety of host–guest properties based on a simple 1-D coordination motif.

(30) The accessible void volume was calculated after the removal of all guest molecules (coordinated, hydrogen-bonding, and free ones) with the program PLATON by using a probe with a radius of 1.2 Å: Spek, A. L. *J. Appl. Crystallogr.* **2003**, *36*, 7–13.

(31) (a) Sekiya, R.; Nishikiori, S. *Chem. Commun.* **2001**, 2612–2613. (b) Sekiya, R.; Nishikiori, S. *Chem.–Eur. J.* **2002**, *8*, 4803–4810. (c) Sekiya, R.; Nishikiori, S.; Ogura, K. *J. Am. Chem. Soc.* **2004**, *126*, 16587–16600.
 (32) (a) Takamizawa, S.; Hiroki, T.; Nakata, E.; Mochizuki, K.; Mori, W. *Chem. Lett.* **2002**, 1208–1209. (b) Takamizawa, S.; Nakata, E.; Saito, T. *Angew. Chem., Int. Ed.* **2004**, *43*, 1368–1371. (c) Takamizawa, S.; Nakata, E.; Yokoyama, H. *Inorg. Chem. Commun.* **2003**, *6*, 763–765. (d) Takamizawa, S.; Saito, T.; Akatsuka, T.; Nakata, E. *Inorg. Chem.* **2005**, *44*, 1421–1424. (e) Takamizawa, S.; Nakata, E.; Saito, T.; Akatsuka, T. *Inorg. Chem.* **2005**, *44*, 1362–1366.
 (33) Yamada, K.; Yagishita, S.; Tanaka, H.; Tohyama, K.; Adachi, K.; Kaizuka, S.; Kumagai, H.; Inoue, K.; Kitaura, R.; Chang, H.-C.; Kitagawa, S.; Kawata, S. *Chem.–Eur. J.* **2004**, *10*, 2647–2660.

Conclusion

In this work, a series of flexible guest-binding coordination polymers generally formulated as $\{[\text{Cu}(\text{bpetha})_2] \cdot 2\text{PF}_6\}_n$ have been synthesized and crystallographically characterized. These have flexible layers constructed from 1-D double chains of $[\text{Cu}(\text{bpetha})_2]_n$, which assemble without any strong interactions. Therefore, they show a propensity for forming various intralayer and interlayer assemblies, and for guest binding, depending on the nature of the Lewis base guest molecules (H_2O , acetone, DMF, MeCN, THF, dioxane, and 2-PrOH in this study). Guests such as acetone, DMF, or MeCN with an sp^2 - or sp -coordinated atom are directly bound at the Cu^{II} centers; in contrast, guests such as THF, dioxane, and 2-PrOH with an sp^3 coordinated atom cannot coordinate to the Cu^{II} centers because of steric hindrance. Instead, these latter guests are incorporated into the host framework by hydrogen bonding and van der Waals interactions. H_2O , with its sp^3 coordinated oxygen, is an exception. Having only small hydrogen atoms around the coordinated oxygen, it can coordinate to spatially restricted Cu^{II} centers. The compound $\{[\text{Cu}(\text{bpetha})_2(\text{acetone})_2] \cdot 2\text{PF}_6\}_n$ (**1**) easily releases its coordinated acetone guests by thermal treatment, forming the stable crystalline host compound $\{[\text{Cu}(\text{bpetha})_2] \cdot 2\text{PF}_6\}_n$, capable of binding guests at the Cu^{II} axial sites protected temporarily by the PF_6^- anions. This desolvated compound again binds acetone guests at the Cu^{II} axial sites when

exposed to acetone vapor, accompanied by a reversible crystal-to-crystal transformation back to **1**. Compound **1** also shows reversible guest-exchange properties involving a color change. We demonstrate that the flexible 1-D coordination polymer with guest-binding Cu^{II} centers is a good candidate for the construction of novel host–guest systems. Future works will investigate the gas and vapor adsorption properties of the desolvated **1**.

Acknowledgment. This work was supported by a Grant-in-Aid for Scientific Research on Priority Areas (No. 434, “Chemistry of Coordination Space”) from the Ministry of Education, Science, Sports, and Culture, Japan. The authors wish to thank the Creative Research Initiative “Sousei”, Hokkaido University, for assistance in obtaining the XPS spectra.

Supporting Information Available: X-ray crystallographic data for **1–6** in CIF format; observed and calculated XRD patterns of **1–6**; TG-DTA results of **1** without guest acetone molecules; IR spectra of **1** without guest acetone molecules; IR spectra of **4'**; N_2 adsorption and desorption isotherms of the desolvated **1**; XRD patterns related to guest exchange between acetone and MeCN; IR spectra of **3'**; photographs of guest-exchanged samples. This material is available free of charge via the Internet at <http://pubs.acs.org>.

IC0609249